



# HHS Public Access

Author manuscript

*Leukemia*. Author manuscript; available in PMC 2018 April 13.

Published in final edited form as:

*Leukemia*. 2018 February ; 32(2): 565–569. doi:10.1038/leu.2017.309.

## Targetable fusions of the FRK tyrosine kinase in ALK-negative anaplastic large cell lymphoma

G Hu<sup>1,\*</sup>, S Dasari<sup>2,\*</sup>, YW Asmann<sup>3</sup>, PT Greipp<sup>1,4</sup>, RA Knudson<sup>4</sup>, HK Benson<sup>1</sup>, Y Li<sup>2</sup>, BW Eckloff<sup>4</sup>, Jin Jen<sup>1</sup>, BK Link<sup>5</sup>, L Jiang<sup>6</sup>, JS Sidhu<sup>7</sup>, LE Wellik<sup>8</sup>, TE Witzig<sup>8</sup>, NN Bennani<sup>8</sup>, JR Cerhan<sup>2</sup>, RL Boddicker<sup>1,#</sup>, and AL Feldman<sup>1,#</sup>

<sup>1</sup>Department of Laboratory Medicine and Pathology, Mayo Clinic, Rochester, MN, USA

<sup>2</sup>Department of Health Sciences Research, Mayo Clinic, Rochester, MN, USA

<sup>3</sup>Department of Health Sciences Research, Mayo Clinic, Jacksonville, FL, USA

<sup>4</sup>Medical Genome Facility, Mayo Clinic, Rochester, MN, USA

<sup>5</sup>Department of Internal Medicine, University of Iowa Hospitals and Clinics, Iowa City, IA, USA

<sup>6</sup>Department of Laboratory Medicine and Pathology, Mayo Clinic, Jacksonville, FL, USA

<sup>7</sup>Department of Pathology and Laboratory Medicine, United Health Services Hospitals, Johnson City/Binghamton, NY, USA

<sup>8</sup>Division of Hematology, Mayo Clinic, Rochester, MN, USA

Anaplastic large cell lymphomas (ALCLs) constitute a group of peripheral (i.e. post-thymic) T-cell non-Hodgkin lymphomas (PTCLs) with overlapping pathologic characteristics, but varying clinical and molecular features. Specifically, ALCLs share cytological and immunophenotypic features, including consistent expression of the lymphocyte activation marker, CD30.<sup>1</sup> The World Health Organization (WHO) classifies ALCLs by their clinical presentation (systemic or cutaneous) and whether or not they bear rearrangements of the anaplastic lymphoma kinase gene, *ALK* (ALK-positive ALCL and ALK-negative ALCL, respectively).<sup>2</sup>

ALK-positive ALCL is characterized by a unique gene expression signature that distinguishes it from ALK-negative ALCL.<sup>3–5</sup> *ALK* rearrangements have a broad spectrum

Users may view, print, copy, and download text and data-mine the content in such documents, for the purposes of academic research, subject always to the full Conditions of use: [http://www.nature.com/authors/editorial\\_policies/license.html#terms](http://www.nature.com/authors/editorial_policies/license.html#terms)

Correspondence and offprint requests to: Rebecca L. Boddicker, Ph.D., Department of Laboratory Medicine and Pathology, Mayo Clinic, 200 First Street SW, Rochester, MN 55905; Phone: 507-284-3805; Fax: 507-284-1599; [boddicker.rebecca@mayo.edu](mailto:boddicker.rebecca@mayo.edu); or Andrew L. Feldman, M.D., Department of Laboratory Medicine and Pathology, Mayo Clinic, 200 First Street SW, Rochester, MN 55905; Phone: 507-284-4939; Fax: 507-284-1599; [feldman.andrew@mayo.edu](mailto:feldman.andrew@mayo.edu).

\*These authors contributed equally to this work

#These authors contributed equally to this work and serve as co-corresponding authors

CONFLICT OF INTEREST: The authors declare no competing financial interests.

### AUTHOR CONTRIBUTIONS

GH contributed to study design and conducted experiments. SD contributed to study design and analyzed data. HKB, JJ, BWE, and LEW conducted experiments. YWA and YL analyzed data. PTG and RAK conducted cytogenetic studies. BKL, JRC, TEW, NNB, JSS, and LJ contributed clinical specimens. RLB and ALF designed the study, analyzed data, and wrote the manuscript.

of functional consequences, prominent among which is activation of the signal transduction protein STAT3.<sup>6</sup> Analogously, STAT3 may be activated in ALK-negative ALCLs by somatic events involving non-*ALK* tyrosine kinase genes, including rearrangements of the *TYK2* or *ROS1* tyrosine kinase genes as well as mutations in *JAK1* or *STAT3* itself.<sup>7, 8</sup> However, the full spectrum of tyrosine kinases involved in ALK-negative ALCL pathogenesis and growth remains incompletely understood, as does the similarity of these events to the molecular signature identified in ALK-positive ALCLs. For example, a subclass of ALK-negative ALCL expressing aberrant transcripts of the *ERBB4* tyrosine kinase gene had a gene expression signature distinct from ALK-positive ALCLs.<sup>9</sup>

To evaluate the relationship between the gene expression profiles of ALK-positive and ALK-negative ALCLs, we performed expression profiling on 31 frozen ALCL tissue samples (Supplementary Table 1) using Affymetrix arrays and derived an ALK signature from our dataset comprising the 29 probes most differentially expressed between these 2 groups (see Supplementary Methods for details). Clustering using this ALK signature identified a single ALK-negative case, ALCL11, which clustered with ALK-positive ALCLs (Figure 1A.i;  $P=0.02$ , Kolmogorov-Smirnov test). The validity of the ALK signature we derived was supported by the presence of multiple genes in common with previously published signatures, including *ALK*, *ARHGEF10*, *ANXA3*, *GALNT2*, *HTRA3*, *IL1RAP*, *MC1R* and *PDE4DIP* (Supplementary Table 2). Furthermore, clustering analysis using previously published ALK-positive ALCL signature genes replicated the unique clustering pattern of ALCL11, but not other ALK-negative ALCLs, with ALK-positive ALCLs (Supplementary Figure 1).

We next used outlier analysis to identify possible non-*ALK* kinase gene overexpression underlying the ALK-like signature in ALCL11. The top kinase genes found to be outliers in this case were fyn related Src family tyrosine kinase (*FRK*) and neurotrophic receptor tyrosine kinase 1 (*NTRK1*; Figure 1A.ii, Supplementary Table 3). *FRK* was expressed exclusively in ALCL11. *NTRK1* was also expressed in 2 cases of ALK-positive ALCL, a disease in which its protein product, TrkA, was recently shown to interact functionally with ALK fusion proteins.<sup>10</sup> To confirm expression of these genes and evaluate this case for potential gene fusions, we performed RNA sequencing in ALCL11. The SnowShoes fusion detection algorithm revealed a novel *CAPRINI-FRK* fusion transcript (Figure 1B, Supplementary Table 4). This fusion was validated by RT-PCR and Sanger sequencing (Supplementary Figure 2A), and the resultant fusion protein was detected by Western blotting in a frozen tissue lysate from ALCL11 (Supplementary Figure 2B).

*FRK*, also called protein tyrosine kinase-5 (*PTK5*), is a member of the BRK family of tyrosine kinases that are related to Src family kinases and similarly possess SH3, SH2, and kinase domains.<sup>11</sup> Of note, the *FRK* and *ALK* regulatory networks share a number of proteins in common, including *STAT3* (Supplementary Table 5). While *FRK* was originally described as a tumor suppressor, recent studies in multiple cancer types have revealed oncogenic genetic events involving *FRK*, including activating mutations in hepatocellular neoplasms and an *ETV6-FRK* fusion in an isolated case of acute myelogenous leukemia (AML).<sup>11–13</sup> Consistent with exon-level *FRK* expression data from RNA sequencing (Supplementary Figure 2C), the sequenced *CAPRINI-FRK* fusion transcript encodes exons

3–8 of *FRK*, with a breakpoint at amino acid 156 in the FRK SH2 domain that leaves the N-terminal kinase domain intact in the resultant fusion protein (Figure 1B). Caprin-1 (*CAPR1*) is a cell cycle-associated protein that is constitutively expressed in lymphocytes,<sup>14</sup> and widely expressed in ALCLs based on our gene expression data (Supplementary Figure 2D). Thus, similar to *NPM1-ALK* and other kinase fusions in ALCL, *CAPRINI-FRK* leads to expression of the tyrosine kinase domain of an otherwise unexpressed protein under control of the active promoter of a constitutively expressed partner gene.

We next developed a novel breakapart fluorescence *in situ* hybridization (BAP-FISH) probe for the *FRK* locus to investigate the frequency and subtype distribution of *FRK* rearrangements in ALCL and other PTCLs (see Supplementary Methods for probe details). BAP-FISH for *FRK* rearrangements was performed on 225 PTCLs and lymphoproliferative disorders, including the original *FRK* fusion case, ALCL11. The original *FRK* rearrangement was validated and additional rearrangements were identified exclusively in ALK-negative ALCLs, with a frequency in this group of 5.4% ( $P = 0.013$ ; Figure 1C; Supplementary Table 6). The ALCLs with *FRK* rearrangements included 5 systemic cases and 1 primary cutaneous case. All were of the so-called “triple-negative” genetic subtype, i.e., in addition to being ALK-negative they lacked rearrangements of *DUSP22* and *TP63*.<sup>15</sup> To assess *FRK* fusion partners further, we then performed dual-fusion FISH for *CAPRINI-FRK* in 5 ALCLs with *FRK* rearrangements and found this fusion only in ALCL11 (Supplementary Table 7). Therefore, we attempted RNA sequencing from paraffin material in these cases; while this approach either failed or was suboptimal in most of the cases, we did identify one case with a *PABPC1-FRK* fusion and another with a possible *MAPK9-FRK* fusion. For both of these events, *FRK* expression began at exon 3, identical to the fusion site observed in *CAPRINI-FRK* (Supplementary Table 7). Because ALK-positive ALCL is associated with favorable outcome,<sup>1</sup> we examined outcomes in ALCLs with *FRK* rearrangements. Indeed, although our series is small, the index case was alive 17 years after diagnosis and 3 of the 4 remaining patients with systemic disease survived at least 5 years (Supplementary Table 8).

To assess the function of *CAPRINI-FRK*, the fusion transcript was cloned from ALCL11 into the pLEX lentiviral expression vector (see Supplementary Materials). We were unable to achieve stable overexpression in ALCL cells, other T-cell lymphoma cell lines, or normal T cells, despite multiple attempts and testing additional expression vectors; this may have been due in part to the large insert size of the *CAPRINI-FRK* fusion transcript. However, we were able to achieve overexpression of *CAPRINI-FRK* in HEK-293T cells and IL3-dependent Ba/F3 cells. The Caprin-1-FRK fusion protein localized primarily to the cytoplasm in HEK-293T cells (Supplementary Figure 3A), consistent with the pattern of FRK immunohistochemical staining in ALCL11 (Figure 1C). In HEK-293T cells, *CAPRINI-FRK* promoted colony formation 2.7-fold over control vector ( $P < 0.001$ ; Figure 2A). Correspondingly, *CAPRINI-FRK* induced STAT3 phosphorylation, which was absent in control cells despite similar levels of total STAT3 (Supplementary Figure 3B). Both effects were somewhat greater than those induced by *NPM1-ALK* in this model. *CAPRINI-FRK* but not *NPM1-ALK* also induced phosphorylation of STAT1 and STAT5, suggesting that *CAPRINI-FRK* may have additional targets not shared by *NPM1-ALK* (Supplementary Figure 3B). Previously published data by Hosoya et al that *ETV6-FRK* did not lead to

phosphorylation of STAT1/3/5/6<sup>13</sup> may reflect differences in cellular context and/or expression of total STAT proteins. In the IL3-dependent Ba/F3 model, both *CAPRINI-FRK* and *NPM1-ALK*, but not control vector, rescued cells from IL3 withdrawal (Figure 2B,C.i). In addition, expression of both *CAPRINI-FRK* and *NPM1-ALK* promoted phosphorylation of STAT3 in the absence of IL3 (Figure 2C.i). We then used the Kinase Inhibitor Resource database (see Supplementary Methods) to identify dasatinib, a tyrosine kinase inhibitor with activity against Src-family and other kinases, as a candidate drug targeting FRK fusions. Indeed, dasatinib inhibited *CAPRINI-FRK*- but not *NPM1-ALK*-driven growth following IL3 withdrawal (Figure 2C.ii), and correspondingly reversed *CAPRINI-FRK*-induced STAT3 phosphorylation (Figure 2C.iii). Conversely, the ALK inhibitor crizotinib specifically inhibited growth in cells expressing *NPM1-ALK* with significantly less effect on *CAPRINI-FRK*-expressing cells (Figure 2C.iv).

In summary, *FRK* rearrangements are recurrent in ALK-negative ALCLs, with a frequency of 5.4% and encompassing both systemic and primary cutaneous subtypes. In the index case, a *CAPRINI-FRK* fusion transcript was discovered and expression of the resultant fusion protein was confirmed. Other fusion partners also exist. *CAPRINI-FRK* promoted phosphorylation of STAT3 and *in vitro* cell growth that could be inhibited by the kinase inhibitor dasatinib. Thus, *FRK* rearrangements represent a novel, candidate therapeutic target in a subset of ALK-negative ALCLs.

## Supplementary Material

Refer to Web version on PubMed Central for supplementary material.

## Acknowledgments

SOURCES OF SUPPORT: Award Numbers R01 CA177734 (ALF), P30 CA15083 (Mayo Clinic Cancer Center), and P50 CA97274 (University of Iowa/Mayo Clinic Lymphoma SPORE) from the National Cancer Institute; CTSA Grant Number UL1 TR000135 from the National Center for Advancing Translational Science (NCATS); Award Number CI-48-09 from the Damon Runyon Cancer Research Foundation (ALF); Department of Laboratory Medicine and Pathology and Center for Individualized Medicine, Mayo Clinic; and the Predolin Foundation.

## References

1. Xing X, Feldman AL. Anaplastic large cell lymphomas: ALK positive, ALK negative, and primary cutaneous. *Adv Anat Pathol*. 2015 Jan.22:29–49. [PubMed: 25461779]
2. Swerdlow SH, Campo E, Pileri SA, Harris NL, Stein H, Siebert R, et al. The 2016 revision of the World Health Organization classification of lymphoid neoplasms. *Blood*. 2016 May 19.127:2375–2390. [PubMed: 26980727]
3. Lamant L, de Reynies A, Duplantier MM, Rickman DS, Sabourdy F, Giuriato S, et al. Gene-expression profiling of systemic anaplastic large-cell lymphoma reveals differences based on ALK status and two distinct morphologic ALK+ subtypes. *Blood*. 2007 Mar 01.109:2156–2164. [PubMed: 17077326]
4. Iqbal J, Wright G, Wang C, Rosenwald A, Gascoyne RD, Weisenburger DD, et al. Gene expression signatures delineate biological and prognostic subgroups in peripheral T-cell lymphoma. *Blood*. 2014 May 08.123:2915–2923. [PubMed: 24632715]
5. Piva R, Agnelli L, Pellegrino E, Todoerti K, Grosso V, Tamagno I, et al. Gene expression profiling uncovers molecular classifiers for the recognition of anaplastic large-cell lymphoma within peripheral T-cell neoplasms. *J Clin Oncol*. 2010 Mar 20.28:1583–1590. [PubMed: 20159827]

6. Chiarle R, Simmons WJ, Cai H, Dhall G, Zamo A, Raz R, et al. Stat3 is required for ALK-mediated lymphomagenesis and provides a possible therapeutic target. *Nat Med*. 2005 Jun.11:623–629. [PubMed: 15895073]
7. Crescenzo R, Abate F, Lasorsa E, Tabbo F, Gaudiano M, Chiesa N, et al. Convergent mutations and kinase fusions lead to oncogenic STAT3 activation in anaplastic large cell lymphoma. *Cancer Cell*. 2015 Apr 13.27:516–532. [PubMed: 25873174]
8. Velusamy T, Kiel MJ, Sahasrabudhe AA, Rolland D, Dixon CA, Bailey NG, et al. A novel recurrent NPM1-TYK2 gene fusion in cutaneous CD30-positive lymphoproliferative disorders. *Blood*. 2014 Dec 11.124:3768–3771. [PubMed: 25349176]
9. Scarfo I, Pellegrino E, Mereu E, Kwee I, Agnelli L, Bergaggio E, et al. Identification of a new subclass of ALK-negative ALCL expressing aberrant levels of ERBB4 transcripts. *Blood*. 2016 Jan 14.127:221–232. [PubMed: 26463425]
10. Shi W, George SK, George B, Curry CV, Murzabdillaeva A, Alkan S, et al. TrkA is a binding partner of NPM-ALK that promotes the survival of ALK+ T-cell lymphoma. *Mol Oncol*. 2017 May 30.
11. Goel RK, Lukong KE. Understanding the cellular roles of Fyn-related kinase (FRK): implications in cancer biology. *Cancer Metastasis Rev*. 2016 Jun.35:179–199. [PubMed: 27067725]
12. Pilati C, Letouze E, Nault JC, Imbeaud S, Boulai A, Calderaro J, et al. Genomic profiling of hepatocellular adenomas reveals recurrent FRK-activating mutations and the mechanisms of malignant transformation. *Cancer Cell*. 2014 Apr 14.25:428–441. [PubMed: 24735922]
13. Hosoya N, Qiao Y, Hangaishi A, Wang L, Nannya Y, Sanada M, et al. Identification of a SRC-like tyrosine kinase gene, FRK, fused with ETV6 in a patient with acute myelogenous leukemia carrying a t(6;12)(q21;p13) translocation. *Genes Chromosomes Cancer*. 2005 Mar.42:269–279. [PubMed: 15611931]
14. Grill B, Wilson GM, Zhang KX, Wang B, Doyonnas R, Quadroni M, et al. Activation/division of lymphocytes results in increased levels of cytoplasmic activation/proliferation-associated protein-1: prototype of a new family of proteins. *J Immunol*. 2004 Feb 15.172:2389–2400. [PubMed: 14764709]
15. Parrilla Castellar ER, Jaffe ES, Said JW, Swerdlow SH, Ketterling RP, Knudson RA, et al. ALK-negative anaplastic large cell lymphoma is a genetically heterogeneous disease with widely disparate clinical outcomes. *Blood*. 2014 Aug 28.124:1473–1480. [PubMed: 24894770]



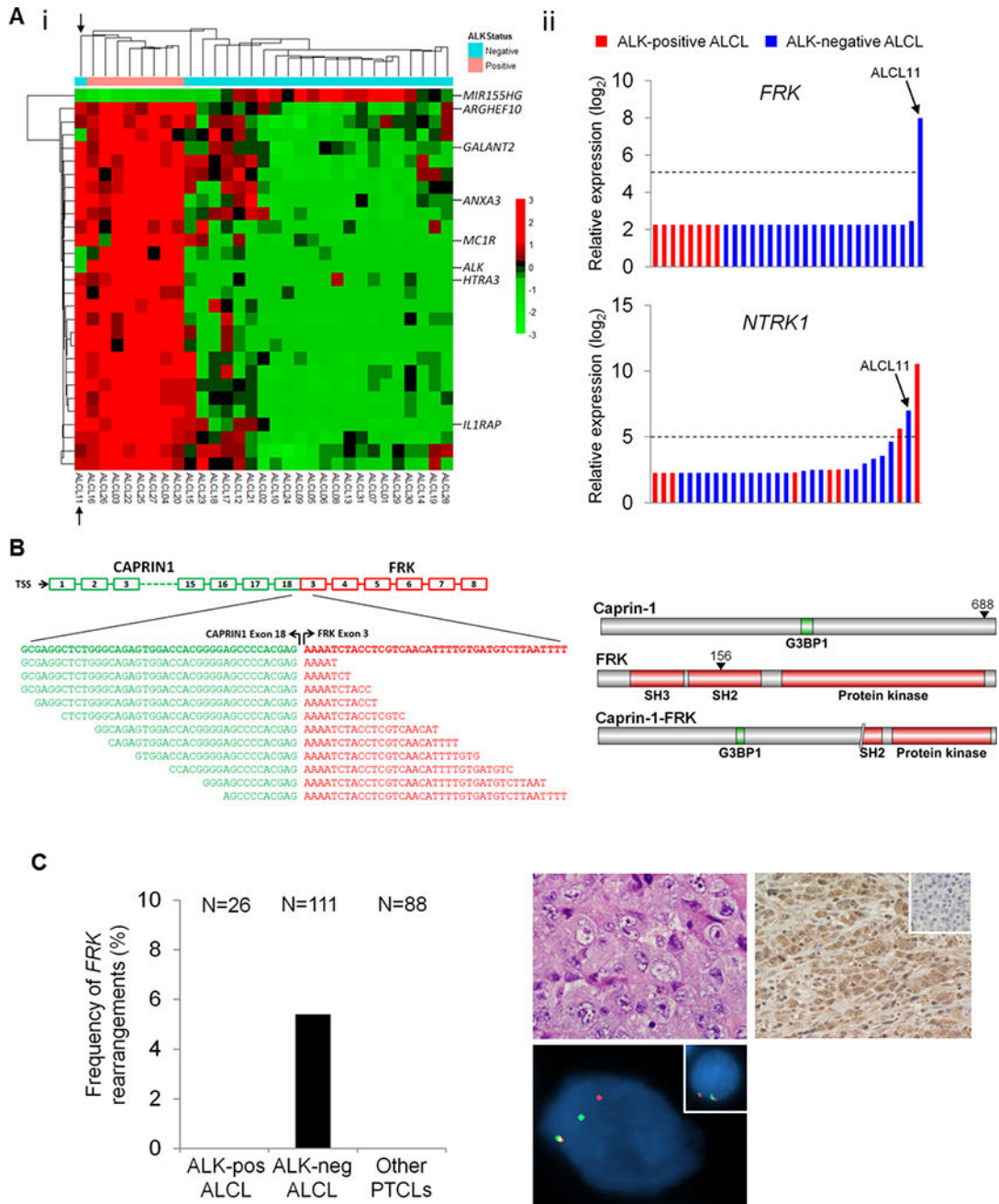


**Figure 1. Discovery of *FRK* rearrangements in ALK-negative ALCL**

A. i. Clustering of 31 ALCLs using 29 probes that most significantly differentiated ALK-positive and ALK-negative ALCL groups (see also Supplementary Table 2). A single ALK-negative ALCL clustered with the ALK-positive cases (ALCL11, arrows). ii. Kinase gene outlier analysis in ALCL11 identified *FRK* and *NTRK1* as the top outlier genes (see also Supplementary Table 3). B. RNA sequencing and fusion detection in ALCL11 identified a chimeric *CAPRIN1-FRK* transcript fusing exon 18 of *CAPRIN1* to exon 3 of *FRK* (see also Supplementary Table 4). The domain structure of the predicted Caprin-1-FRK fusion protein resulting from the identified *CAPRIN1-FRK* transcript is shown at right. C. FISH evaluation

of 225 PTCLs showed *FRK* rearrangements in 5.4% of ALK-negative ALCLs and not in any other PTCL subtype (see also Supplementary Table 5). Top center image, hematoxylin and eosin stain of ALCL11 (original magnification,  $\times 1000$ ). Top right image, immunohistochemical staining for *FRK* was present in ALCL11; inset: staining is absent in an ALK-positive case without an *FRK* rearrangement (ALCL26; see also Supplementary Figure 2B; original magnification,  $\times 400$ ). Bottom center image, FISH in ALCL11 using a breakapart probe to the *FRK* locus showed one normal red-green fusion signal and abnormal separation of the remaining red and green signals; inset: signal pattern in a normal cell showing two fusion signals (original magnification,  $\times 600$ ).

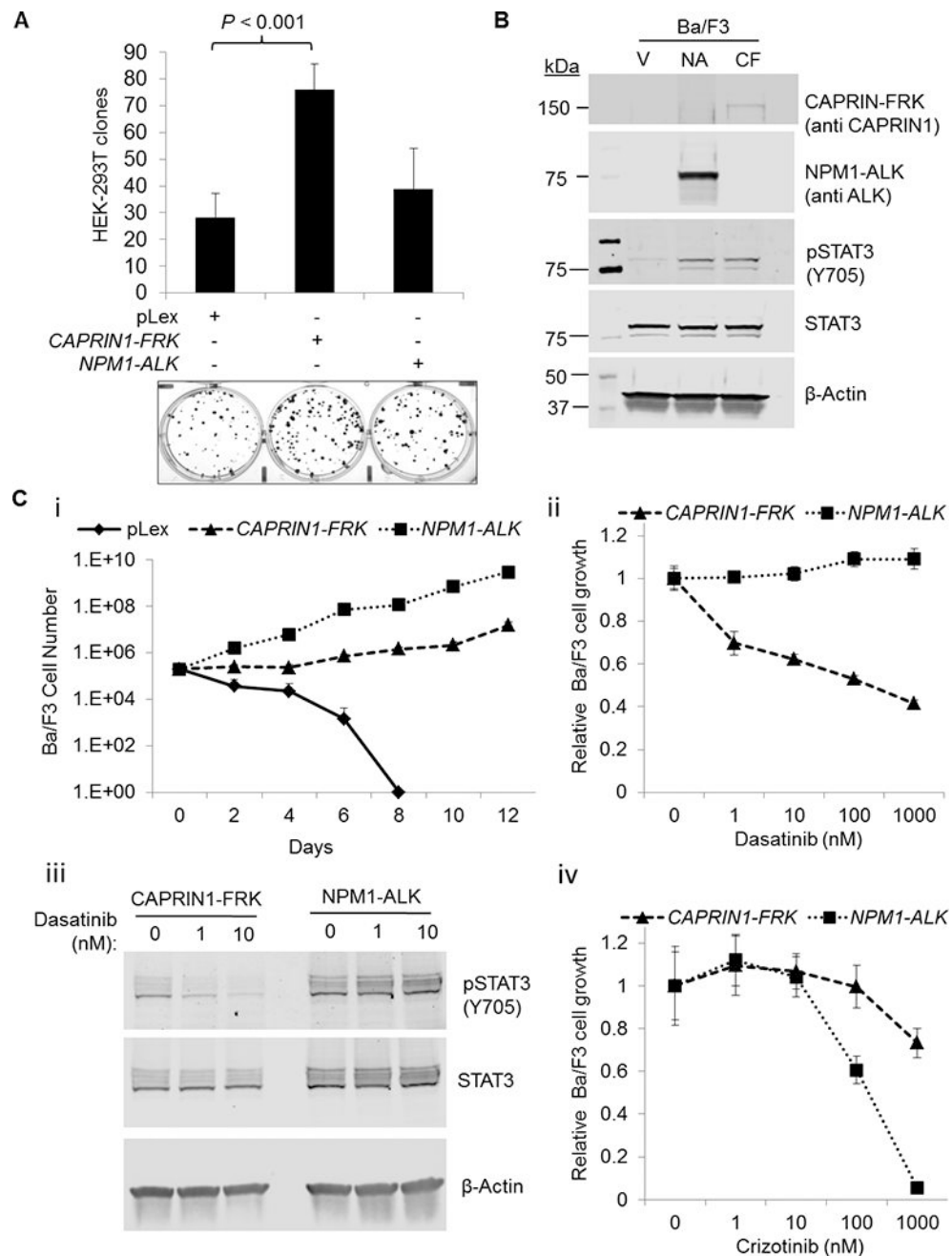


**Figure 2. Function and targetability of CAPRINI-FRK**

A. *CAPRINI-FRK* promoted colony formation 2.7-fold in HEK-293T cells compared to empty vector (pLex;  $P < 0.001$ ). Cells expressing *NPM1-ALK* also are shown. B. Ba/F3 cells were cultured in the absence (48 h withdrawal) of IL3 followed by analysis by Western Blot. *CAPRINI-FRK* (as well as *NPM1-ALK*) induced STAT3 phosphorylation at Y705 in Ba/F3 cells (V, empty vector; NA, *NPM1-ALK*; CF, *CAPRINI-FRK*). C. i. *CAPRINI-FRK* and *NPM1-ALK* rescued IL3-dependent Ba/F3 cells from IL3 withdrawal. ii. The tyrosine kinase inhibitor dasatinib targeted *CAPRINI-FRK* but not *NPM1-ALK* in Ba/F3 cells. iii. A dose-dependent inhibition of pSTAT3 was observed in *CAPRINI-FRK*-expressing cells but



not in cells expressing NPM1-ALK. iv. The ALK inhibitor crizotinib targeted *NPM1-ALK* but was relatively ineffective in inhibiting Ba/F3 cells expressing *CAPRINI-FRK*.

Author Manuscript

Author Manuscript

Author Manuscript

Author Manuscript